J|A|C|S
ARTICLES
Published on Web 03/27/2002

The s−p Bonded Representatives of the Prominent $BaAl_4$ Structure Type: A Case Study on Structural Stability of Polar Intermetallic Network Structures

Ulrich Häussermann,*,† Shahrad Amerioun,† Lars Eriksson,‡ Chi-Shen Lee,§ and Gordon J. Miller*,§

Contribution from the Department of Inorganic Chemistry and the Department of Structural Chemistry, Stockholm University, S-10691 Stockholm, Sweden, and the Department of Chemistry, Iowa State University, Ames, Iowa 50011

Received October 19, 2001

Abstract: This work presents a detailed, combined experimental and theoretical study on the structural stability of s−p bonded compounds with the $BaAl_4$ structure type (space group *I*4/*mmm*, Z = 2) as part of a broad program to investigate the complex questions of structure formation and atomic arrangements in polar intermetallics. From ab initio calculations employing pseudopotentials and a plane wave basis set, we extracted optimized structural parameters, binding energies, and the electronic structure of the systems $AeX(III)_4$, $AeX(II)_2X(IV)_2$, $AeX(II)_2X(III)_2$ (Ae = Ca, Sr, Ba; X(II) = Mg, Zn; X(III) = Al, Ga; X(IV) = Si, Ge). For all systems we found a pronounced pseudo-gap in the density of states separating network X_4^{2-} bonding from antibonding electronic states that coincides with the Fermi level for an electron count of 14 electrons per formula unit, the optimum value for stable $BaAl_4$-type polar intermetallics. However, the synthesis and structural characterization (from X-ray single crystal and powder diffraction data) of the new compounds $AeZn_{2-\delta}Al_{2+\delta}$, $AeZn_{2-\delta}Ga_{2+\delta}$ (Ae = Ca, Sr, Ba; $\delta = 0-0.2$) and $AeMg_{0.9}Al_{3.1}$, $AeMg_{1.7}Ga_{2.3}$ (Ae = Sr, Ba) manifested that electron deficiency is rather frequent for $BaAl_4$-type polar intermetallics. The site preference for different "X" elements in the ternary systems was quantified by calculating "coloring energies", which, for some systems, was strongly dependent on the size of the electropositive Ae component. The Ae^{2+} cations decisively influence the nearest neighbor distances in the encapsulating polyanionic networks X_4^{2-} and the structures of these networks are surprisingly flexible to the size of the Ae component without changing the overall bonding picture. A monoclinically distorted variant of the $BaAl_4$ structure occurs when the cations become too small for matching the size of encapsulating X_4^{2-} cages. An even larger size mismatch leads to the formation of the $EuIn_4$ structure type.

Introduction

Chemical systems at the boundary region of different bonding types are usually distinguished by an extraordinarily large variety of different structure types and special physical properties. The family of polar intermetallics, which represent the link between s−p bonded metallic and s−p bonded, salt-like, valence compounds, makes no exception. Polar intermetallics form between electropositive alkali, alkaline earth, or rare earth metals with the metallic elements from the triel (Group 13: Al, Ga, In, Tl) and tetrel groups (Group 14: Sn, Pb) and their systematic exploration in recent years has revealed a wealth of novel and peculiar structures.[1−6] The p-elements are formally reduced by the electropositive component and form clusters or networks based on localized multicenter bonding, thus unravelling the complicated bonding patterns in the region between valence compounds (i.e. Zintl phases) with two-center localized bonding and close-packed arrangements with completely delocalized bonding. Corbett has exploited the full potential of this idea for the synthesis of polar intermetallics by investigating ternary and quaternary systems with either differently sized electropositive components or different p-elements, or p-elements partly replaced by the electronegative divalent metals Zn and Cd.[5,6] The important findings of his group include the following: (i) usually the p-elements attempt to realize multicenter bonded clusters and networks which fit the electron count of the p-elements in their particular reduced state. However, a significant number of polar intermetallics exhibit small deviations from the optimum electron count (excessive for clusters and deficient for networks); (ii) the kind and concentration of the electropositive component governs the kind of polyanionic p-element structure (clusters or networks) through the differ-

* Corresponding author. E-mail: gmiller@iastate.edu.
† Department of Inorganic Chemistry, Stockholm University.
‡ Department of Structural Chemistry, Stockholm University.
§ Department of Chemistry, Iowa State University.

(1) Belin, C.; Tillard-Charbonnel, M. *Prog. Solid State Chem.* **1993**, *22*, 59.
(2) Belin, C.; Tillard-Charbonnel, M. *Coord. Chem. Rev.* **1998**, *180*, 529.
(3) Cordier, G.; Eisenmann, B. *Chemistry, Structure And Bonding of Zintl Phases And Ions*; Kauzlarich, S., Ed.; VCH: New York, 1996; pp 61−137.
(4) Fässler, T. F.; Hoffmann, S. *Z. Kristallogr.* **1999**, *214*, 722.
(5) Corbett, J. D. *Angew. Chem., Int. Ed.* **2000**, *39*, 670.
(6) Corbett, J. D. *Chemistry, Structure and Bonding of Zintl Phases and Ions*; Kauzlarich, S., Ed.; VCH: New York, 1996; pp 139−18.

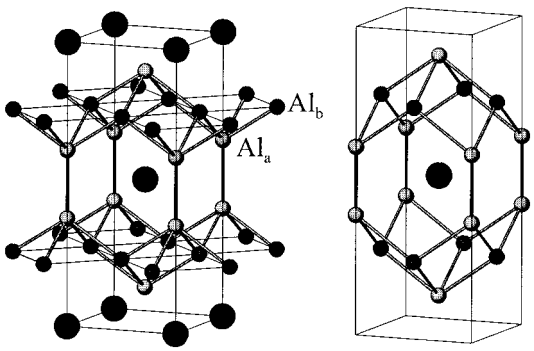

Figure 1. The $BaAl_4$ structure. Large spheres denote the Ba atoms, small spheres the Al atoms (two different sites: dark, Al_b; light, Al_a). On the right-hand side the Fedorov coordination polyhedron surrounding each Ba atom is outlined.

ences in the Madelung energy contributions between cations and the different polyanion types; and (iii) optimum packing between cations and the polyanionic part is an important ingredient to the stability of a particular structure. These results emphasize the difference between polar intermetallics and valence compounds, because, for the latter, electron count almost exclusively governs their structural stability (point (i) above). For polar intermetallics these three criteria of structural stability are intimately related. As recently pointed out by Seo and Corbett,[7] it is the mutual optimization of the Madelung energy and space filling which can override the usually dominating factor of electron count, which leads to the observed deviations from the optimum values of electron count for many compounds. However, the complicated interplay of the factors determining structural stability in polar intermetallics has not been quantified yet.

In this article we elaborate on these complex questions by analyzing the $BaAl_4$ structure type in detail. Although the $BaAl_4$ structure is widely adopted among intermetallic compounds,[8,9] we confined our investigation to the homogeneous group of s−p bonded representatives corresponding to polar intermetallics. Due to its simplicity and the rather large number of s−p bonded representatives, this structure type may be regarded as a prototype for polar intermetallics with a polyanionic network structure. The $BaAl_4$ structure features a body-centered tetragonal unit cell (space group *I*4/*mmm*, No. 139) where the Ba atoms occupy the corner and center positions and the Al atoms form a $^3_\infty[Al_4]^{2-}$ network (Figure 1). This network contains two independent sites: the basal Al atoms (Al_b) occupy the Wyckoff site 4d ($^1/_2$, 0, $^1/_4$) and form two-dimensional square nets which are alternately capped above and below the plane by the apical Al atoms (Al_a) occupying the Wyckoff site 4e (0, 0, *z*). The resulting layers of square pyramids are connected by bonds between the Al_a atoms to yield the final network $^3_\infty[Al_4]^{2-}$. The second bonding contact in this network is the distance between Al_a and Al_b atoms, whereas the distance between two Al_b atoms in the square net is long and nonbonding. Thus, each Al_b atom is surrounded nearly tetrahedrally by four Al_a atoms and each Al_a atom is surrounded by four Al_b atoms and one Al_a in a square pyramidal fashion. The coordination polyhedron for the Ba atoms corresponds to an 18-vertex (space filling) Fedorov polyhedron[10] defined by one set of Al_b atoms (8) and two sets of Al_a atoms (8 and 2, respectively). However, the second set of Al_a atoms is distinctly farther away from the center of the Fedorov polyhedron. Thus a coordination number of 16 seems to be more appropriate for the Ba atoms.

The s−p bonded $BaAl_4$-type family comprises the binary compounds $SrAl_4$, $EuAl_4$, $BaAl_4$, $SrGa_4$, $EuGa_4$, $BaGa_4$, and $BaIn_4$, i.e., they possess the same valence electron count of 14 electrons per formula unit. Zheng and Hoffmann[11] and Burdett and Miller[12] developed a clear bonding picture for these compounds. They suggested two-center, two-electron (2c2e) bonds between the layer connecting apical atoms and multicenter (5c6e) bonding in the pyramids between one apical and four basal network atoms. Per formula unit one 2c2e and two 5c6e bonds occur, thus yielding an optimum electron count of 14. This bonding model holds as well for $CaAl_4$ and $CaGa_4$, which adopt a monoclinically distorted variant of the $BaAl_4$ type.[13] With two different elements occupying the two network sites, ternary compounds with the $BaAl_4$-type (also described as the $ThCr_2Si_2$ structure type) are obtained. (The $CaBe_2Ge_2$ structure is another ternary variant of the $BaAl_4$-type family but involves a different decoration pattern of the elements,[14] and will not be discussed in this paper. Aspects of its bonding and stability with respect to the $ThCr_2Si_2$-type have been addressed by Zheng.[15]) The corresponding s−p bonded compounds may now be divided into 14-electron systems (with four known representatives: $CaZn_2Ge_2$, $SrZn_2Ge_2$, $BaMg_2Si_2$, and $BaMg_2Ge_2$) and electron-deficient 12-electron systems (just one reported compound: $CaAl_2Zn_2$). (The Zn-containing compounds are considered as exclusively s−p bonding because of the low-lying 3d states in elemental Zn.[16,17]) When writing the formula unit for ternary compounds we use the sequence $Ae(X_b)_2(X_a)_2$, which we keep throughout this article. The electropositive (electron-donating) component, which represents one of the heavier alkaline earth metals Ca, Sr, or Ba, is collectively expressed as Ae and the network-forming atoms as X.

The purpose of our work is to study the variations of the polyanionic network in $BaAl_4$-type polar intermetallics (and the associated changes in the electronic structure) as a function of electron count, network polarity, and size of the Ae component. In particular, we report the synthesis and structural characterization of the new, electron-deficient representatives $SrAl_2Zn_2$, $BaAl_2Zn_2$, $CaZn_2Ga_2$, $SrZn_2Ga_2$, $BaZn_2Ga_2$, $SrMg_2Ga_2$, and $BaMg_2Ga_2$, as well as that of the solid solutions $SrMg_xAl_{4-x}$ and $BaMg_xAl_{4-x}$ ($x_{max} \approx 0.8$). Additionally we reexamined the binary compounds $SrAl_4$, $BaAl_4$, $SrGa_4$, and $BaGa_4$ where, with the exception of $SrAl_4$, structural characterization was based solely on X-ray powder film methods performed several decades ago. We accompanied the experimental work by ab initio density functional calculations using pseudopotentials and a plane wave basis set.

(7) Seo, D.-K.; Corbett, J. D. *J. Am. Chem. Soc.* **2000,** *40*, 9621−9627.
(8) Pearson, W. B. *J. Less-Common Met.* **1985**, *109*, L3.
(9) Pearson, W. B. *J. Solid State Chem.* **1985**, *56*, 278.
(10) von Federov, J. S. *Z. Kristallogr.* **1904**, *38*, 321.
(11) Zheng, C.; Hoffmann, R. *Z. Naturforsch.* **1986**, *41b*, 292.
(12) Burdett, J. K.; Miller, G. J. *Chem. Mater.* **1990**, *2*, 12.
(13) Miller, G. J.; Li, F.; Franzen, F. *J. Am. Chem. Soc.* **1993,** *115*, 3739−3745.
(14) Daniuk, S.; Jarlborg, T.; Kontrym-Sznajd, G.; Majsnerowski, J. *Condens. Matter* **1989,** 8397.
(15) Eisenmann, B.; May, N.; Müller, W.; Schäfer, H. *Z. Naturforsch. B* **1972**, *27*, 1155−1157.
(16) Zheng, C. *J. Am. Chem. Soc.* **1993**, *115*, 1047−1051.
(17) Häussermann, U.; Simak, S. I. *Phys. Rev. B* **2001**, *64*, 245114.

Experimental Section

Synthesis. The materials $AeAl_2Zn_2$ and $AeZn_2Ga_2$ (Ae = Ca, Sr, Ba) and $AeAl_4$, $AeGa_4$, $AeMg_xAl_{4-x}$ ($x = 0.33, 0.67, 1.0, 1.2$), $AeMg_2Ga_2$ (Ae = Sr, Ba) were prepared from the elements and handled in an Ar-filled glovebox (O_2 concentration <10 ppm). The pure elements, Ba granulates (ABCR, 99.9%), Sr granulates (ABCR, 99.9%), Mg granulates (ABCR, 99.9%), Al ingots (Aldrich, 99.9%), Ga rod (ABCR, 99.9%) and Zn powder (ABCR, 99.9%), were weighed in either Nb or Ta ampules which were sealed and placed in fused silica Schlenk tubes under reduced pressure. Reactant mixtures were heated to 800−850 °C for 24 h to ensure complete melting, followed by either slow cooling (at a rate of 5 °C/h) or rapid quenching to room temperature and subsequent annealing. The samples were annealed for four weeks at a temperature of 500 ×bcC (Al-containing mixtures) and 600 ×bcC (Ga containing mixtures), which improved considerably crystal quality and homogeneity of the products. All products, which were highly crystalline and exhibited a silvery, metallic luster, were characterized by Guinier powder diagrams (Cu Kα; Si standard). The composition of the ternaries (with the exception of the materials $AeAl_2Zn_2$) was analyzed with the EDX (energy-disperse X-ray) method in a JEOL 820 scanning electron microscope averaging between 5 and 10 analyses for each sample. In $AeMg_xAl_{4-x}$ (Ae = Sr, Ba; $x = 1.0$) we observed, apart from the $BaAl_4$-type compound, the occurrence of other products. The amount of these, yet unidentified, products increased for $x = 1.2$. The 2θ values of the $BaAl_4$-type compound were found to be virtually identical in both samples, suggesting that the maximum amount of Mg (x) in the solid solutions $AeMg_xAl_{4-x}$ is slightly below $x = 1.0$. From EDX analyses of numerous $BaAl_4$-type crystals from the samples $AeMgAl_3$ we obtained the limiting compositions $SrMg_{0.9(1)}Al_{3.1(1)}$ and $BaMg_{0.86(2)}Al_{3.14(2)}$. For $AeMg_2Ga_2$ (Ae = Sr, Ba), EDX analyses revealed a loss of Mg in the $BaAl_4$-type products and we obtained $AeMg_{1.7(1)}Ga_{2.3(1)}$. The composition of the materials $AeAl_2Zn_2$ was determined from Zn/Al site occupancy refinements of X-ray data sets from several single crystals from each product. We observed that a strict Zn/Al molar ratio of 1 is just possible for Ae = Ca and that small deviations occur for Ae = Sr, Ba (i.e. $AeAl_{2+\delta}Zn_{2-\delta}$ with $\delta \approx 0.1$ for Ae = Sr and $\delta \approx 0.2$ for Ae = Ba). Studies of $AeAl_xZn_{4-x}$, $x > 2$, were also carried out and will be reported elsewhere.[18] For $AeZn_2Ga_2$ the Zn/Ga molar ratio was also found to be slightly below 1: $AeZn_{1.8(1)}Ga_{2.2(1)}$ (EDX analyses).

Structure Determination The lattice constants of the investigated $BaAl_4$-type systems were obtained from least-squares refinement of measured and indexed lines of the corresponding Guinier powder diffractograms.[19] To ensure proper assignment of the indices the observed lines were compared with the calculated ones[20] by using the positional parameters resulting from the structure refinements. Single-crystal intensity data were collected at 293 K from at least two different crystals from each of the samples $AeAl_4$, $AeGa_4$, $AeMgAl_3$ (Ae = Sr, Ba), $AeZnAl_3$ (Ae = Sr, Ba), $BaMg_2Ga_2$, and $AeAl_2Zn_2$ (Ae = Ca, Sr, Ba) on a STOE IPDS or Rigaku AFC6R diffractometer with monochromatic Mo Kα radiation ($\lambda = 0.71073$ Å). All data sets were corrected for Lorentz and polarization effects. Absorption correction was performed either by the program X-shape[21] as included in the STOE IPDS software or with the aid of the average of ι-scans of three reflections at different 2θ values. For structure refinement (full-matrix least-squares on F^2) the program SHELXL97[22] was used. The structure refinement of the materials $SrMg_2Ga_2$ and $AeZn_2Ga_2$ (Ae = Ca, Sr, Ba) (single-phase samples) was performed from X-ray powder diffraction data that were collected on a STOE STADI powder diffractometer at 293 K (equipped with a position-sensitive detector (PSD)) with monochromatic Cu Kα radiation ($\lambda = 1.54056$ Å) in transmission mode. Due to absorption problems, the measurement of the $BaZn_2Ga_2$ sample was repeated in reflection mode. Rietveld refinement was carried out using the program FULLPROF.[23] Summaries of the data collections and refinements are listed in Table 1. Additional crystallographic data are given in the Supporting Information.

Calculational Details Total energy calculations for the systems $AeX(III)_4$, $AeX(II)_2X(IV)_2$, $AeX(IV)_2X(II)_2$, $AeX(II)_2X(III)_2$, and $AeX(III)_2X(II)_2$ (Ae = Ca, Sr, Ba; X(II) = Mg, Zn; X(III) = Al, Ga; X(IV) = Si, Ge) were performed within ab initio density functional theory as implemented in the program VASP.[24−26] This program allows molecular dynamics simulations (and structure relaxations) using pseudopotentials and a plane-wave basis set. The Kohn−Sham equations were solved self-consistently using an iterative matrix diagonalization method and an efficient Pulay mixing scheme of the charge density. In our systems we relaxed the free parameter of the atomic position 4e (0, 0, z) simultaneously with the c/a ratio for a set of constant volumes until forces converged to less than 0.005 eV/Å. In a second step we extracted the equilibrium volume and ground-state energy by fitting the E vs V values to the Murnaghan equation of state.[27] Concerning the pseudopotentials, ultrasoft Vanderbilt-type pseudopotentials[28,29] were employed and the actual valence electrons of the elements involved are indicated in the following configurations: Mg $3s^2$, Ca $4s^2$, Sr $4p^65s^2$, Ba $5p^66s^2$, Al $3s^23p^1$, Si $3s^23p^2$, Zn $3d^{10}4s^2$, Ga $3d^{10}4s^24p^1$, and Ge $4s^24p^2$. The exchange and correlation energy was assessed by the generalized gradient approximation (GGA) according to Perdew and Wang.[30] Convergency was checked with respect to the plane-wave cutoff and the number of **k**-points used in the summation over the Brillouin zone. For systems consisting of elements with just s and p valence electrons, we found a cutoff of 200 eV to be sufficient, whereas for systems containing elements with d pseudo-core electrons, the cutoff was increased to 300 eV. The **k**-points were obtained by the Monkhorst−Pack method[31] and sampled on a dense grid of 15 × 15 × 15.

Results

The binary aluminides with the $BaAl_4$ structure ($SrAl_4$ and $BaAl_4$) were already reported over 60 years ago,[32,33] but the structure of $SrAl_4$ was recently redetermined by Göbel et al.[34] The binary gallides $SrGa_4$ and $BaGa_4$ were synthesized and structurally characterized by Bruzzone in 1965.[35] We reexamined the lattice constants and the positional coordinate of the X_a sites for $SrAl_4$, $BaAl_4$, $SrGa_4$, and $BaGa_4$. In comparing our measured lattice constants with the literature values, the differences are rather small for the gallides and $SrAl_4$, whereas we see a considerable difference of the c axis for $BaAl_4$. Concerning the z parameter of the X_a sites, our values obtained from single-crystal X-ray refinements are generally greater than those obtained from X-ray powder film methods ($BaAl_4$, $SrGa_4$, and $BaGa_4$).

(18) Lee, C.-S. Experimental and Theoretical Investigations in Alkaline Earth−Zinc−Aluminum Intermetallic Systems, Ph.D. Thesis, Iowa State University, 2000.
(19) Werner, P.-R. *Ark. Kemi* **1969**, *31*, 513−516.
(20) Yvon, K.; Jeitschko, W.; Parthé, E. *J. Appl. Crystallogr.* **1977**, *10*, 73.
(21) *X-shape*: Crystal Optimisation for Numerical Absorption correction. STOE & Cie Gmbh: Darmstadt, Germany 1996.
(22) Sheldrick, G.; *SHELXL-97*: Program for Crystal Determination; University of Göttingen: Göttingen, Germany, 1997
(23) Rodriguez-Carvajal, J. *FULLPROF* (version 2k): Program for Rietveld Analysis of Neutron and X-ray Powder Diffraction Data; Laboratoire Leon Brillouin: CEA-Saclay, France, 2000.
(24) Kresse, G.; Hafner, J. *Phys. Rev.* **1993**, *B47*, RC 558.
(25) Kresse, G.; Furthmüller, J. *Phys. Rev.* **1996**, 11169.
(26) Kresse, G.; Furthmüller, J. *Comput. Mater. Sci.* **1996**, *6*, 15.
(27) Murnaghan, F. D. *Finite Deformation of an Elastic Solid*; Wiley: New York, 195.
(28) Vanderbilt, D. *Phys. Rev.* **1990**, *B41*, 7892.
(29) Kresse, G.; Hafner, J. *J. Phys.: Condens. Matter.* **1994**, *6*, 824.
(30) Perdew, J. P.; Wang, Y. *Phys. Rev.* **1992**, *B45*, 13244.
(31) Monkhurst, H. J.; Pack, J. D. *Phys. Rev.* **1973**, *B13*, 518.
(32) Nowotny, H.; Wesenberg, H. *Z. Metallkd.* **1939**, *31*, 363−364.
(33) Andress, K. R.; Alberti, E. *Z. Metallkd.* **1935**, *27* (6), 126−128.
(34) Göbel, S.; Somer, M.; Carillo-Cabrera, W.; Peters, E.-M.; von Schnering, H. G. *Z. Kristallogr.* **1996**, *211*, 18.
(35) Bruzzone, G. *Acta Crystallogr.* **1965**, *18*, 113−132.

Table 1. Selected Data Collection and Refinement Parameters for the $BaAl_4$-Type Systems Investigated (lattice parameters from Guinier powder patterns)

empirical formula	$SrAl_4$	$BaAl_4$	$SrGa_4$	$BaGa_4$	$CaZn_{2.0(1)}$, $Al_{2.00}$[a]	$SrZn_{1.94(3)}$, $Al_{2.06(3)}$[a]	$BaZn_{1.84(4)}$, $Al_{2.16(4)}$[a]	$CaZn_{1.8(1)}$, $Ga_{2.2(1)}$[b]	$SrZn_{1.9(6)}$, $Ga_{2.2(1)}$[b]	$BaZn_{1.8(5)}$, $Ga_{2.2(5)}$[b]	$SrMg_{0.9(1)}$, $Al_{3.1(1)}$[b]	$BaMg_{0.86(2)}$, $Al_{3.14(2)}$[b]	$SrMg_{1.7(1)}$, $Ga_{2.3(1)}$[b]	$BaMg_{1.7(1)}$, $Ga_{2.3(1)}$[b]
formula wt	195.54	245.25	366.50	416.21	224.80	270.00	315.91	310.28	357.82	407.53	193.14	242.95	275.68	325.39
space group, Z	*I4/mmm*, 2	*I4/mmm*, 2	*I4/mmm*, 2	*I4/mmm*, 2	*I4/mmm*, 2	*I4/mmm*, 2	*I4/mmm*, 2	*I4/mmm*, 2	*I4/mmm*, 2	*I4/mmm*, 2	*I4/mmm*, 2	*I4/mmm*, 2	*I4/mmm*, 2	*I4/mmm*, 2
a /Å	4.4637(2)	4.5680(5)	4.4454(3)	4.5645(4)	4.122(1)	4.2172(9)	4.4602(9)	4.2011(4)	4.3536(4)	4.5186(3)	4.4464(3)	4.6260(6)	4.5447(5)	4.7029(9)
c /Å	11.2129(6)	11.2896(18)	10.7432(12)	10.7757(13)	11.512(8)	11.417(4)	11.376(5)	11.0310(16)	10.9187(13)	10.9359(12)	11.2118(13)	11.4473(19)	11.7917 (2)	11.6593(41)
volume /Å^3	223.42(2)	235.58(5)	212.31(3)	224.51(4)	195.60(10)	208.28(9)	226.30(10)	194.69(4)	206.80(3)	220.97(3)	223.43(4)	244.97(6)	243.55(6)	257.88(11)
z_a	0.3836(3)	0.3812(1)	0.3830(1)	0.3796(2)	0.3919(1)	0.3874(1)	0.3812(1)	0.3870(1)	0.3830(1)	0.3767(2)	0.3875(1)	0.3842(1)	0.3933(1)	0.3895(2)
SOF(X_a)	1 Al	1 Al	1 Ga	1 Ga	0.10(3) Al, 0.90 Zn	0.18(1) Al, 0.82 Zn	0.33(1) Al, 0.67 Zn	0.55 Ga, 0.45 Zn	0.55 Ga, 0.45 Zn	0.55 Ga, 0.45 Zn			1 Ga	1 Ga
SOF(X_b)	1 Al	1 Al	1 Ga	1 Ga	0.89(2) Al, 0.11 Zn	0.85(1) Al, 0.15 Zn	0.75(1) Al, 0.25 Zn	0.55 Ga, 0.45 Zn	0.55 Ga, 0.45 Zn	0.55 Ga, 0.45 Zn			0.12(3) Ga, 0.88 Mg	0.08(2) Ga, 0.92 Mg
refinement method	*f*	*f*	*f*	*f*	*f*	*f*	*f*	*f*	*g*	*g*	*f*	*f*	*g*	*f*
d_{calc} (g/cm^3)	2.91	3.46	5.73	6.16	3.82	4.33	4.64	5.29	5.75	6.12	2.87	3.29	3.76	4.19
R-values	0.032,[c] 0.053[d]	0.009,[c] 0.022[d]	0.0276,[c] 0.0457[d]	0.029,[c] 0.083[d]	0.020,[c] 0.040[d]	0.029,[c] 0.042[d]	0.014,[c] 0.032[d]	0.0518,[c] 0.0565[e]	0.0389,[c] 0.0418[e]	0.0606,[c] 0.0845[e]	0.0168,[c] 0.0379[d]	0.0066,[c] 0.0149[d]	0.0552,[c] 0.0763[e]	0.0347,[c] 0.1193[d]

[a] X-ray refined composition. [b] EDX determined composition. [c] $R1 = \sum||F_o| - |F_c||/\sum|F_o|$. [d] $wR2 = [\sum[w(F_o^2 - F_c^2)^2]/\sum[w(F_o^2)^2]]^{1/2}$, $w = \sigma_F^{-2}$. [e] R-bragg $= [\sum[(I_o^2 - I_c^2)^2]/\sum[(I_o^2)^2]]^{1/2}$. [f] Single crystal least squares. [g] Rietveld least squares.

In ternary compounds two different elements occupy the network (X_b and X_a sites) and the site occupancies create another structural parameter. There are four reported representatives of 14-electron ternary compounds with the $ThCr_2Si_2$-type arrangement, $CaZn_2Ge_2$,[36] $SrZn_2Ge_2$,[37] $BaMg_2Si_2$,[38] and $BaMg_2Ge_2$,[38] which were not the subject of our experimental investigation. For 12-electron compounds, we were able to extend the number of representatives considerably beyond just the single reported example, $CaAl_2Zn_2$,[39] to $AeX(II)_2X(III)_2$ (Ae = Sr, Ba; X(II) = Mg, Zn; X(III) = Al, Ga). $CaAl_2Zn_2$ was reported with the basal position (X_b) occupied exclusively by Al and the apical one (X_a) by Zn.[39] However, our investigations reveal the occurrence of mixed occupation to a minor degree (X_b: 89%Al/11%Zn; X_a: 90%Zn/10%Al). With the heavier alkaline earth metals Sr and Ba in $AeAl_2Zn_2$, this trend becomes even more pronounced: the apical and basal sites show increasing "disorder". Furthermore, the Zn/Al mole ratio drops below 1, i.e., becomes richer in Al, as the alkaline earth metal changes from Ca to Ba. In particular, Zn occupancy on the apical site decreases from 91% to 66% whereas it increases on the basal site from 10% to 25%. The $AeZn_2Ga_2$ system behaves differently in this respect. Although our EDX analyses show the Zn/Ga molar ratio to be slightly below 1 (0.9), there is no significant influence of the Ae component on the composition. However, it is not possible to extract the site distribution from X-ray refinements. Based on the findings of our theoretical calculations (see below), we assume both sites randomly occupied by Zn and Ga. Concerning the 12-electron systems, "$AeMg_2Al_2$" and "$AeMg_2Ga_2$", we excluded Ae = Ca from our synthetic work because $CaAl_4$ and $CaGa_4$ do not adopt the $BaAl_4$ structure type at ambient temperature. According to our experiments, the compounds "$SrMg_2Al_2$" and "$BaMg_2Al_2$" do not exist: the maximum amount of Mg in $AeMg_xAl_{4-x}$ was found to be ca. $x = 0.9$, which corresponds to a Mg/Al mole ratio of 0.29. This is in contrast to "$AeMg_2Ga_2$" where the compounds $SrMg_{2-\delta}Ga_{2+\delta}$ and $BaMg_{2-\delta}Ga_{2+\delta}$ ($\delta = 0.3$), with a Mg/Ga mole ratio of 0.74, could be prepared. For $SrMg_{0.9}Al_{3.1}$ and $BaMg_{0.9}Al_{3.1}$ the site distribution of Mg on the two network positions could not be extracted satisfactorily from X-ray refinements. Again, the results of the theoretical calculations were very helpful in the assignment because they reveal a clear preference for Mg to occupy the basal position. Mg clearly occupies this site in "$SrMg_2Ga_2$" and "$BaMg_2Ga_2$".

Results from the theoretical calculations are graphically summarized in Figures 2−4, and are also tabulated in the Supporting Information. Figure 2 illustrates the trends in energy differences between ternary pairs $Ae(X1_b)_2(X2_a)_2$ and $Ae(X2_b)_2(X1_a)_2$ with opposite distributions of the elements X1 and X2 on the network positions as Ae varies from Ca to Ba, e.g., $\Delta E = E(AeZn_2Al_2) - E(AeAl_2Zn_2)$ is plotted. In the following, we call this energy difference the "coloring energy" and it is always positive, i.e., relative to the lower energy arrangement of atoms. Figures 3 and 4 display respectively the parameters V and c/a for the theoretical equilibrium (lowest energy) structures together with the experimental values. We observe a

(36) Eisenman, B.; May, N.; Müller, W.; Schäfer, H.; Weiss, A.; Winter, J.; Ziegleder, G. *Z. Naturforsch.* **1970**, *25B*, 1350−1352.
(37) Dörrscheidt, W.; Niess, N.; Schäfer, H. *Z. Naturforsch.* **1976**, *31B*, 890−891.
(38) Eisenmann, B.; Schäfer, H. *Z. Anorg. Allg. Chem.* **1974**, *403*, 163−172.
(39) Cordier, G.; Czech, E.; Schäfer, H. *Z. Naturforsch.* **1984**, *39B*, 1629−1632.

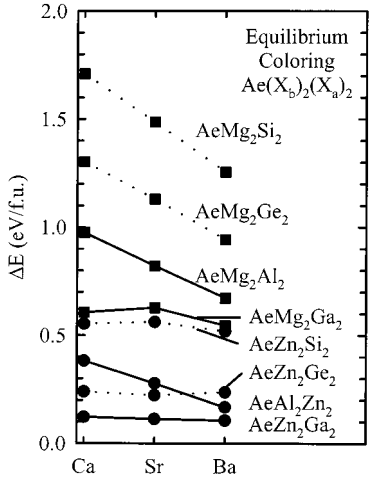

Figure 2. Calculated energy differences (coloring energies) between the equilibrium structures of $Ae(X1)_2(X2)_2$ and $Ae(X2)_2(X1)_2$ (Ae = Ca, Sr, Ba) with the formula written as $Ae(X_b)_2(X_a)_2$: dashed lines connect 14-electron systems, solid lines connect 12-electron systems, squares label ternary Mg systems, circles label ternary Zn systems.

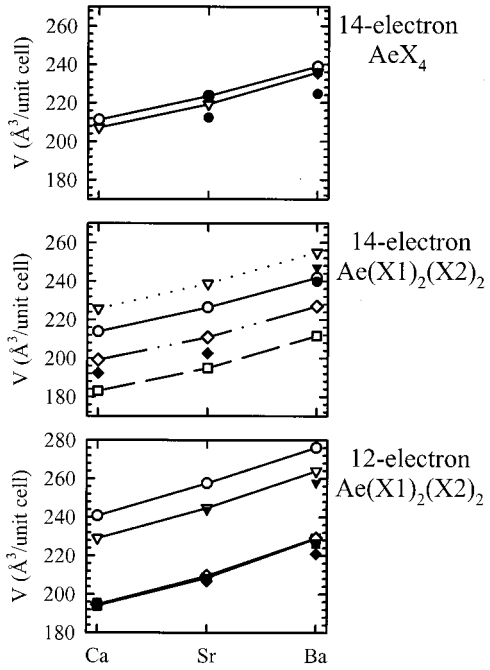

Figure 3. Variations in the unit cell volume (Å^3) in the systems $Ae(X1)_2(X2)_2$ (Ae = Ca, Sr, Ba). Open symbols represent calculated values, filled symbols correspond to the experimental values of the known compounds. (Top) 14-electron binary compounds $AeAl_4$ (circles) and $AeGa_4$ (triangles). (Middle) 14-electron ternary compounds $AeMg_2Si_2$ (circles), $AeMg_2Ge_2$ (triangles), $AeZn_2Si_2$ (squares), and $AeZn_2Ge_2$ (diamonds). (Bottom) 12-electron ternary compounds $AeMg_2Al_2$ (circles), $AeMg_2Ga_2$ (triangles), $AeAl_2Zn_2$ (diamonds), and $AeZn_2Ga_2$ (squares).

remarkably good agreement between experimental and theoretical values. Even the ground-state volumes, which are difficult to reproduce with density functional methods, are within a 2% range of deviation for Al- or Si-containing compounds and differ up to 5% from the experimental value for systems containing Ga or Ge. For $AeAl_2Zn_2$, we notice an increasing deviation between experimental and computed structural parameters as Ae changes from Ca to Ba. This is in accord with the experimental observation of increasing mixed occupancy of Zn and Al atoms on the two network sites and the increasing deviation of the Zn/Al mole ratio from 1. The increasing

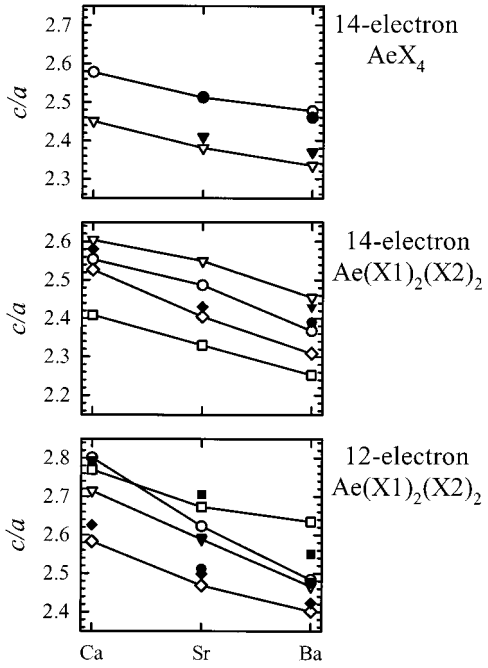

Figure 4. Variations in the *c/a* ratio in the systems $Ae(X1)_2(X2)_2$ (Ae = Ca, Sr, Ba). Open symbols represent calculated values, filled symbols correspond to the experimental values of the known compounds. (Top) 14-electron binary compounds $AeAl_4$ (circles) and $AeGa_4$ (triangles). (Middle) 14-electron ternary compounds $AeMg_2Si_2$ (circles), $AeMg_2Ge_2$ (triangles), $AeZn_2Si_2$ (squares), and $AeZn_2Ge_2$ (diamonds). (Bottom) 12-electron ternary compounds $AeMg_2Al_2$ (circles), $AeMg_2Ga_2$ (triangles), $AeAl_2Zn_2$ (diamonds), and $AeZn_2Ga_2$ (squares).

occupational disorder corresponds to the decreasing energy difference between $AeAl_2Zn_2$ and $AeZn_2Al_2$ with increasing size of Ae (cf. Figure 2). For Ae = Ca the coloring energy is 0.38 eV/formula unit and decreases to just 0.17 eV/formula unit for Ae = Ba. Also, for $AeZn_2Ga_2$ the deviations between experimental and computed structural parameters are rather large. Here, we see a very small (Ae independent) coloring energy between $AeGa_2Zn_2$ and $AeZn_2Ga_2$ of about 0.11 eV/formula unit with $AeZn_2Ga_2$ the preferred distribution. From this, we assume that Zn and Ga randomly occupy the network sites in the synthesized products, which is further supported by the fact that the experimental structural parameters *c/a* and z_a are between the theoretical ones for ordered $AeZn_2Ga_2$ and $AeGa_2Zn_2$.

Finally, the structural parameters in Figures 3 and 4 vary roughly in a linear way—*V* increases while *c/a* decreases (z_a also decreases but is not shown)—when Ae changes from Ca to Ba. Especially noteworthy is the amount of constant volume increase for the different systems because it matches almost perfectly the differences in the volumes of the ions Ae^{2+} according to the volume increment table established by Biltz[40] ($V(Ca^{2+})$ = 10.8 Å^3, $V(Sr^{2+})$ = 18.3 Å^3, $V(Ba^{2+})$ = 26.6 Å^3), yielding differences of 15 Å^3 and 16.6 Å^3 between Ca and Sr compounds and between Sr and Ba compounds, respectively. This finding matches well the conception of polar intermetallics as composed of an oxidized electropositive component (here the heavier alkaline earth metals) and a polyanionic (reduced) network (or cluster arrangement).

(40) Biltz, W. *Raumchemie der festen Stoffe*; Verlag Leopold Voss: Leipzig, 1934 (in German).

Table 2. Electronegativities of the Network Atoms in the s−p Bonded Representatives of the $BaAl_4$-Type (AR = Allred−Rochow) and SEN Values for Various $AeX1_2X2_2$ Systems Investigated

EN	AR	Pauling
Mg	1.2	1.2
Al	1.5	1.5
Si	1.7	1.8
Zn	1.7	1.6
Ga	1.8	1.6
Ge	2.0	1.8
Mg/Al	0.3	0.3
Mg/Si	0.5	0.6
Mg/Ga	0.6	0.4
Mg/Ge	0.8	0.6
Al/Zn	0.2	0.1
Zn/Si	0	0.2
Zn/Ga	0.1	0
Zn/Ge	0.3	0.2

Discussion

Site Preferences. In ternary compounds with the $ThCr_2Si_2$ structure two different kinds of atoms are distributed on the positions of the three-dimensional network, which represents the coloring or site preference problem in its simplest form.[41] Previous theoretical studies based on Mulliken population analyses obtained from semiempirical tight-binding calculations[11] suggest that elements with greater electronegativity prefer to occupy the apical (X_a) site rather than the basal (X_b) site. A look at the calculated coloring energies from our ab initio calculations for the 14-electron and 12-electron ternary systems shown in Figure 2 supports the simple picture of the electronegativity governing site preference. However, the magnitudes of the coloring energy do not necessarily correlate with the differences in electronegativity. This is especially the case for Zn-containing systems where the electronegativity differences are very low (see Table 2), but the differences in the coloring energies are quite variable. Generally, the site preference problem for the s−p bonded representatives of the $BaAl_4$-type appears to be more intricate than just being related to electronegativity differences. For some systems, the Ae component strongly influences site preference on the polyanionic network, i.e., the coloring energy decreases with increasing size of Ae. Electron count may also affect the magnitude of the coloring energy because for 12- and 14-electron systems with comparable electronegativity differences (Ae/Mg/Ga − Ae/Mg/Si and Ae/Zn/Ga − Ae/Zn/Si), the 12-electron systems display a lower coloring energy (and, therefore, a lower tendency to order) than the 14-electron systems.

Electronic Structure Changes and Variations in the Network. **(a) 14-Electron Binary Systems.** The densities of states (DOS) and valence electron densities of the 14-electron, binary compounds, $AeAl_4$ and $AeGa_4$, in their calculated equilibrium structures are shown, respectively, in Figures 5 and 6. The overall shapes of the DOS curves of the six compounds are very similar, and show a pronounced pseudo-gap at or very close to the Fermi level. This pseudo-gap separates bonding from antibonding states.[11,12] It is a characteristic feature in the DOS of many polar intermetallics and a consequence of strong covalent bonding (orbital overlap) in the polyanionic structures. When the Fermi level coincides with the pseudo-gap, the particular system has an optimum electron count with all bonding states occupied (however, among polar intermetallics deviations from an optimum electron count are rather frequent), which often allows a localized bonding description for the polyanionic structure. As already mentioned, for the $^3_\infty[Al_4]^{2-}$ and $^3_\infty[Ga_4]^{2-}$ networks in $AeAl_4$ and $AeGa_4$, the localized bonding description in terms of 5c6e multicenter bonding within the pyramids and 2c2e bonds connecting the pyramid layers after refs 11 and 12 exists. The valence electron densities in the (100) plane of these compounds (Figure 6) support this elegant bonding picture: (i) the covalently bonded $^3_\infty[X_4]^{2-}$ networks are manifested in the projection and (ii) the different types of bonds (2c2e X_a-X_a and 5c6e X_b-X_a) are discernible. The 2c2e X_a-X_a bond shows higher values of valence electron density than the 5c6e X_b-X_a bonds, but need not mean shorter distances: in $BaAl_4$, the calculated Al_a-Al_a and Al_b-Al_a distances are nearly equal (Al_a-Al_a, 2.71 Å (the experimental value is 2.684(5) Å) vs Al_b-Al_a, 2.73 Å (the experimental value is 2.722(1) Å)).

Next, we analyze the variations of the network distances as a function of Ae (see Figure 7a). The shortest network X−X distances naturally occur in the Ca systems, where the distances of the 2c2e bonds (Al_a-Al_a, 2.54 Å; Ga_a-Ga_a, 2.47 Å) correspond well to the values of single-bonded pairs.[42] Thus, for $CaAl_4$ and $CaGa_4$ the volume of the unit cell is determined by the $^3_\infty[Al_4]^{2-}$ and $^3_\infty[Ga_4]^{2-}$ networks, which achieve equilibrium covalent bond lengths for 2c2e bonded pairs $(X_a)_2$ and 5c6e bonded pyramids $X_a(X_b)_4$. With increasing size of the Ae, the polyanionic network has to expand and, surprisingly, it is the distance of the 2c2e X_a-X_a bonds that is most flexible and increases from 2.54 to 2.71 Å and from 2.47 to 2.66 Å in $AeAl_4$ and $AeGa_4$, respectively. The corresponding increases in the distances of the multicentered X_b-X_a bonds is from 2.66 to 2.73 Å ($AeAl_4$) and from 2.63 to 2.71 Å ($AeGa_4$). Nevertheless, the electronic structures of AeX_4 show minor changes from Ae = Ca to Ba that are connected to the overall increase of the $^3_\infty[X_4]^{2-}$ network distances: increasing network distances imply a decreasing s−p bandwidth (the bottom of the valence bands rises by 0.7 eV with respect to the Fermi level when going from CaX_4 to BaX_4) and, as a consequence of the weaker interactions between the network atoms, the width of the pseudo-gap diminishes as well. This is also reflected in the electron density between bonded pairs of network atoms, which decreases somewhat when going from CaX_4 to BaX_4 (Figure 7).

For the Ae−X distances, which are available as Supporting Information, the shorter $Ae-X_a$ distances increase faster with increasing size of Ae than $Ae-X_b$ and become comparable in value in the Ba compounds. Thus, the Ae coordination polyhedron becomes increasingly spherical when going from the Ca to the Ba compounds. As mentioned earlier, Ae coordination plays an important role for the stability of polar intermetallic compounds. In particular, $CaAl_4$ and $CaGa_4$ do not crystallize in the tetragonal $BaAl_4$-type, but in a monoclinically distorted derivative of this structure.[13] A possible reason for this distortion is an electronic instability that arises from an insufficient coordination of the Ca^{2+} ions in the tetragonal

(41) Miller, G. *Eur. J. Inorg. Chem.* **1998**, 523.

(42) Pauling, L. *The Nature of the Chemical Bond*; Cornell University Press: New York, 1960.

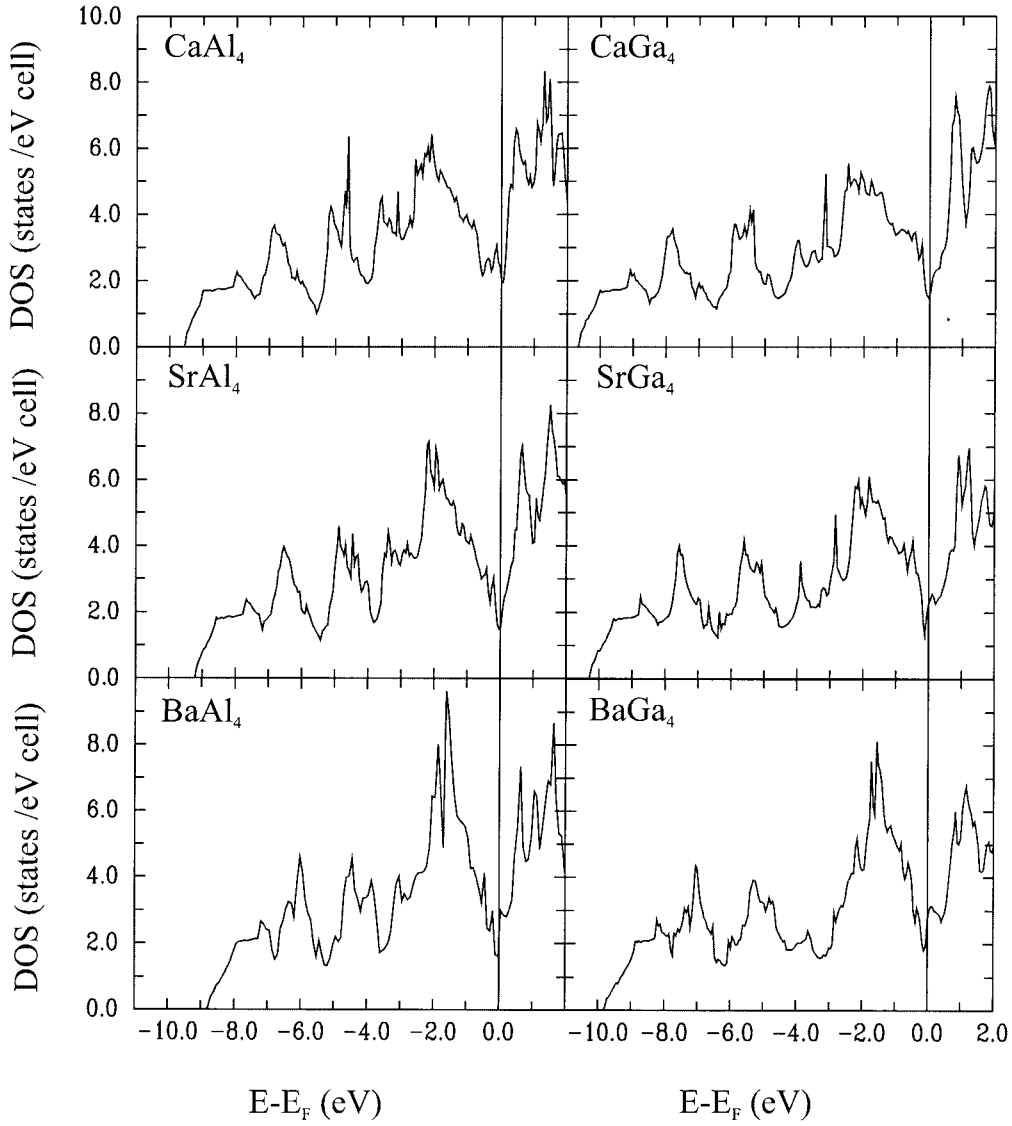

Figure 5. Densities of states of the $BaAl_4$-type 14-electron binary compounds. Energies shown with respect to the calculated Fermi level.

$^3_\infty[X_4]^{2-}$ network. Apparently, this network is quite flexible to encapsulate the differently sized Ae atoms, especially via the variable 2c2e bonded X_a-X_a distances. However, for the Ca compounds the tetragonal network attains minimum X−X distances corresponding to equilibrium covalent bond lengths. Consequently, the size of the resulting cages for Ca might be too large for sufficient coordination thus driving a distortion to a lower symmetric structure. We return to this point in a later section.

(b) 14-Electron Ternary Systems. In the 14-electron, ternary representatives of the $BaAl_4$-type, a divalent metal (Mg or Zn) occupies the X_b sites of the polyanionic network and an element from the tetrel group (Si or Ge) occupies the X_a sites. To gain a first impression of the change of the electronic structure when the homonuclear $^3_\infty[X_4]^{2-}$ network turns into a heteronuclear $^3_\infty[(X1)_2(X2)_2]^{2-}$ one, we consult the valence electron density distributions in $SrMg_2Si_2$, $SrMg_2Ge_2$, $SrZn_2Si_2$, and $SrZn_2Ge_2$ (see Figure 8). (Due to the small changes in ρ when altering the Ae component, we take the Sr compounds as representatives for all Ae compounds.) In the heteronuclear networks a transfer of electronic charge between X1 and X2 is possible. The $^3_\infty[Mg_2X_2]^{2-}$ networks appear as decomposed into Mg^{2+} cations and X_2^{6-} dimeric Zintl anions, which are isoelectronic to the halogen dumbbells. This gives the impression that the Mg compounds actually might correspond to semiconducting, valence compounds (Zintl phases). On the other hand, the electronegativity differences between the network atoms in $^3_\infty[Zn_2X_2]^{2-}$ are much lower and the valence electron density distribution suggests polar covalent bonding within the polyanionic networks. However, comparing ρ for Mg and Zn compounds must be done cautiously: core electron density appears in the plots because Zn 3d electrons are included in the calculations, but core density is missing at the Mg atoms.

The DOS reveals a more detailed picture of the actual bonding situation. There are two distinguishable differences between the DOS for the ternaries, $AeMg_2Si_2$ and $AeMg_2Ge_2$ (Figure 9a), and the isoelectronic binaries, $AeAl_4$ and $AeGa_4$ (Figure 5): (i) the valence s bands of the more electronegative network atom are energetically detached from the remaining bands and are split and (ii) the pseudo-gap, which is either at or close to the Fermi level, is broader but more shallow (above 2 states per eV per cell). The latter finding contradicts an ionic description of the network ($Mg^{2+} + X_2^{6-}$) and, indeed, the DOS of $AeMg_2Si_2$ and $AeMg_2Ge_2$ have a considerable contribution from Mg

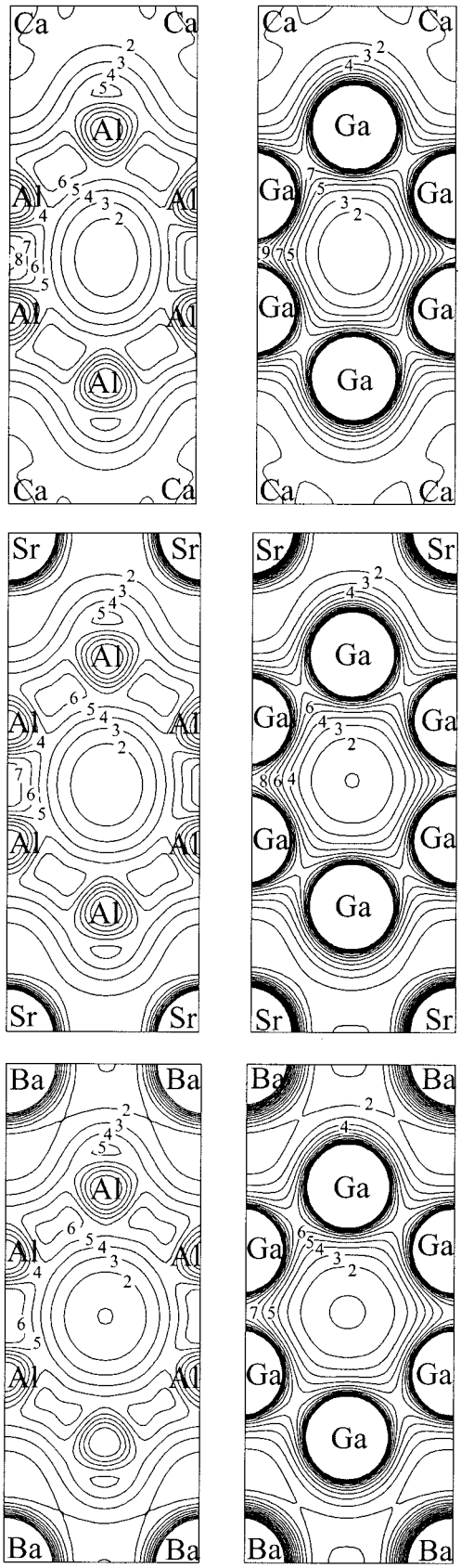

Figure 6. Valence charge distribution in the (100) plane of the $BaAl_4$-type 14-electron binary compounds. The charge distribution is presented in a range between 0.0 and 0.8 $e^-/Å^3$ with contours $n \times 0.04$ $e^-/Å^3$.

3s and 3p states for bands within ca. 5 eV below the Fermi level.[43] The separation and splitting of the Si and Ge s bands in

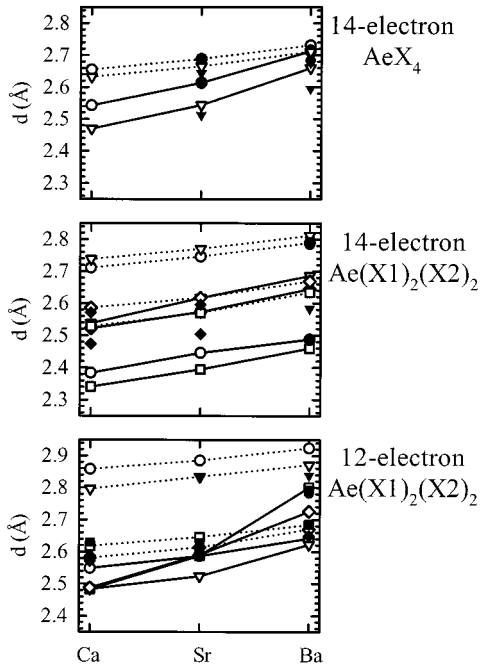

Figure 7. Variations in the interatomic distances X_a-X_a (solid lines) and X_a-X_b (dotted lines) in the investigated systems $Ae(X_b)_2(X_a)_2$ (calculated equilibrium structures). Open symbols represent calculated values, filled symbols correspond to the experimental values of the known compounds. (Top) 14-electron binary compounds $AeAl_4$ (circles) and $AeGa_4$ (triangles). (Middle) 14-electron ternary compounds $AeMg_2Si_2$ (circles), $AeMg_2Ge_2$ (triangles), $AeZn_2Si_2$ (squares), and $AeZn_2Ge_2$ (diamonds). (Bottom) 12-electron ternary compounds $AeMg_2Al_2$ (circles), $AeMg_2Ga_2$ (triangles), $AeAl_2Zn_2$ (diamonds), and $AeZn_2Ga_2$ (squares).

the DOS of the Mg compounds arise from the mismatch between the (low lying) s orbital energies of the more electronegative atoms on the apical position and the (high lying) 3s and 3p orbital energies of Mg in the basal position. Thus, the interaction between Si/Ge valence s orbitals with the Mg 3s/3p orbitals is diminished and, instead, they form σ_g and σ_u orbital combinations within X_a-X_a pairs. Their dispersion, however, arises from interactions with Mg orbitals: their bandwidths, which are between 1 and 2 eV, are lowest for the Ba compounds where the X_a-Mg distances are largest.

The DOS curves of the Zn compounds in Figure 9b are very similar to those of the corresponding Mg compounds, except for the occurrence of Zn 3d states that are well localized at ca. 7.5 eV below the Fermi level. They are confined to a narrow 1.5 eV range (as in elemental Zn[17]) and do not decisively interfere with the network s−p bonding. There is also separation and splitting of the X_a s bands, but the interaction between X_a p and Zn 4s/4p orbitals is somewhat stronger than that between X_a p and Mg 3s/3p ones, as indicated by the slightly larger dispersion of the bands in the part of the DOS above the Zn 3d bands up to the Fermi level. This dispersion is around

(43) It is possible to calculate site projected densities of states from a plane wave basis set when defining spheres around the atomic sites. The sum of the volume of the spheres must be the same as the unit cell volume. However, there is no unambiguous way to define sphere radii in binary (and ternary) systems. We chose the relative sizes of the atom-centered spheres according to the positions of the saddle points of superpositioned Hartree potentials of the neutral atoms as provided from the program TB-LMTO 4.6 (van Schilfgarde, M.; Paxton, T. A.; Jepsen, O.; Krier, G.; Burkhard, A.; Andersen, O. K. *Program TB-LMTO*, 4.6; Max-Planck Institut, Stuttgart: Stuttgart, 1994). We found that the number of states (integrated partial DOS up to the Fermi level) of the Mg sites in the ternary compounds $AeMg_2Si_2$ and $AeMg_2Si_2$ (Ae = Ca, Sr, Ba) amount to between 15 and 25% of the total number of states.

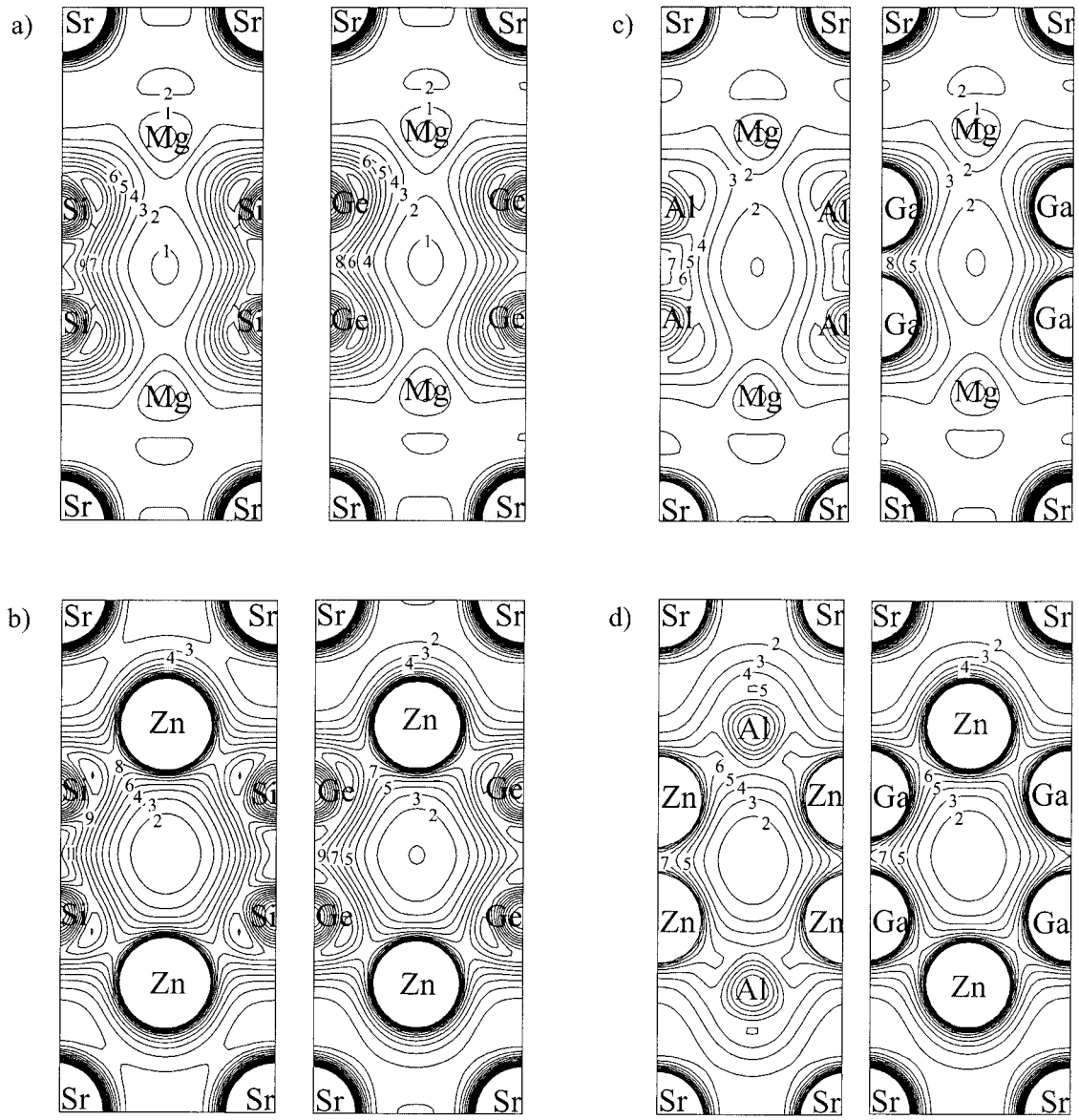

Figure 8. Valence charge distributions in the (100) plane of the 14-electron and 12-electron ternary compounds $Sr(X_b)_2(X_a)_2$: (a) $SrMg_2Si_2$; (b) $SrZn_2Si_2$; (c) $SrMg_2Al_2$; and (d) $SrAl_2Zn_2$. The charge distributions are presented in a range between 0.0 and 0.8 $e^-/Å^3$ with contours $n \times 0.04$ $e^-/Å^3$.

6 eV compared to about 5 eV in the Mg compounds. Therefore, bonding in the heteronuclear networks $^3_\infty[Mg_2X_2]^{2-}$ and $^3_\infty[Zn_2X_2]^{2-}$ is not so different as might have been expected from the electron density distributions. If the $^3_\infty[X_4]^{2-}$ networks of the binary compounds are considered to be covalently bonded, those in the ternaries have a substantial ionic contribution. It is a matter of taste to distinguish bonding in $^3_\infty[Zn_2X_2]^{2-}$ and $^3_\infty[Mg_2X_2]^{2-}$ and describe the former as a polar covalent network and the latter as a polarized ionic one. The most important point is that because of the high polarizing power of Mg^{2+}, a complete ionic description of the networks $^3_\infty[Mg_2X_2]^{2-}$ in terms of Mg^{2+} and X_2^{6-} (in the spirit of the Zintl–Klemm concept) is not appropriate.

Finally, compared to the binary alkaline earth–triel compounds AeX_4, the 2c2e bonded X_a-X_a contacts between tetrel atoms in $AeMg_2X_2$ and $AeZn_2X_2$ are considerably shorter than the X_a-X_b distances (see Figure 7b). Both types of distances are well separated and increase by ca. 0.1 Å from Ca to Ba compounds. Thus, contrary to the 2c2e pairs of triel atoms in the binaries, the lengths of the 2c2e bonded contacts of tetrel atoms in the ternary compounds are less variable. For Ae = Ca the X_a-X_a distances agree well with the value of single bonded pairs (in the elemental diamond structures of Si and Ge, the Si–Si and Ge–Ge distances are 2.35 and 2.45 Å, respectively. Note, the agreement between experimental and theoretical distances is worse for Ge systems than for the Si systems.) The trend in the Ae–X distances in the ternaries is similar to that in the binaries: the shorter $Ae-X_a$ distances increase more with increasing size of Ae than the $Ae-X_b$ ones and both distances become comparable in the Ba systems.

(c) 12-Electron Ternary Systems. Experimentally known are the eight compounds $AeAl_2Zn_2$, $AeZn_2Ga_2$, $SrMg_{2-\delta}Ga_{2+\delta}$, and $BaMg_{2-\delta}Ga_{2+\delta}$ ($\delta = 0.3$) (this work). Compared to the 14-electron systems the electronegativity differences between the network atoms are lower and the coloring energies are smaller. Therefore, in 12-electron systems the divalent component may preferentially occupy the apical position as found in $AeAl_2Zn_2$. Moreover, in 12-electron compounds the situation of optimum

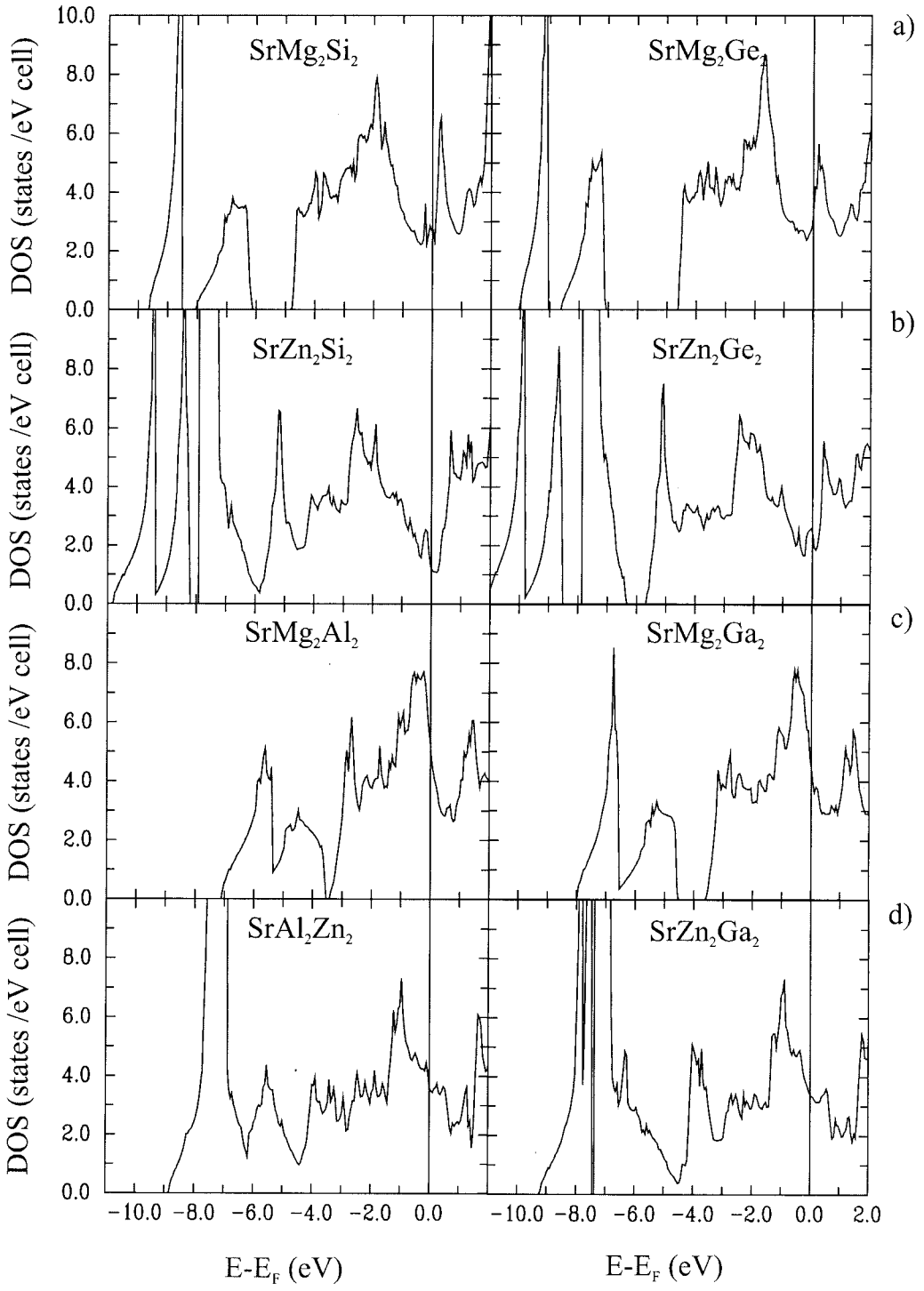

Figure 9. Densities of states of (a) the Mg-containing $BaAl_4$-type, 14-electron ternary compounds; (b) the Zn-containing $BaAl_4$-type 14-electron ternary compounds; (c) the Mg-containing $BaAl_4$-type 12-electron ternary compounds; and (d) the Zn-containing $BaAl_4$-type 12-electron binary compounds. Energies are shown with respect to the calculated Fermi level.

electron count is lost and the corresponding networks become electron deficient. In the DOS curves (shown in Figure 9, parts c and d, for the Mg and Zn compounds, respectively) the pseudo-gap is now situated above the Fermi level. Interestingly, for most of these compounds the Fermi level (corresponding to a band filling of 12 electrons per formula unit) is just above a steep change in the DOS, which suggests that a further decrease of electron count would lead to a considerable electronic destabilization due to a large DOS at the Fermi level. This agrees with the experimental observation that 12 electrons per formula unit presents the lower limit of electron count for these s−p bonded, $BaAl_4$-type representatives. Otherwise, the DOS curves of the 12-electron ternaries are remarkably similar to those of the corresponding 14-electron ones. With the exception of $AeAl_2Zn_2$, the separation of the valence s bands of the apical atoms from the bulk DOS is less pronounced than in the 14-electron ternary compounds. The valence electron density distributions (Figure 8) within the polyanionic networks for both the Mg and the Zn compounds appear less polarized than ρ in the corresponding 14-electron ternaries.

The X_a-X_b distances increase linearly by about 0.1 Å when going from Ca to Ba (see Figure 7c). The trend in the X_a-X_a distances is more complicated. For the Zn compounds these 2c2e contacts are very flexible: within $AeZn_2Ga_2$ the X_a-X_a distance increases by 0.23 Å (Ga−Ga contacts) and within $AeAl_2Zn_2$ by 0.32 Å (Zn−Zn contacts). Consequently, the X_a-X_a distance becomes longer than X_a-X_b for $BaAl_2Zn_2$ and $BaZn_2Ga_2$. The nonlinear rise of the Zn_a-Zn_a distances in $AeAl_2Zn_2$ further indicates that the $^3_\infty[Al_2Zn_2]^{2-}$ network becomes too small for encapsulating Ba^{2+}, which is supported by the experimental fact that "$BaAl_2Zn_2$" actually cannot be obtained but rather $BaAl_{2.2}Zn_{1.8}$ (Zn/Al mole ratio of 0.82). For the Mg compounds the variations in the X_a-X_a distances appear much smaller than in the Zn compounds due to larger unit cells (i.e. network sizes) in the Mg examples, which allows relaxation of the 2c2e X_a-X_a contacts.

To summarize the trends in network distances for the three classes of compounds with increasing size of the Ae component (Figure 7), changes of the X_a-X_b distances are rather small and very similar for all systems, whereas the X_a-X_a distances readily adapt to the size of Ae. The flexibility of the 2c2e contacts is lowest for pairs of tetrel atoms and highest for a pair of divalent Zn atoms. The trends in the Ae−X distances are similar for all classes. An essential question concerning the 12-electron (electron deficient) ternaries is whether the reduction of electron count might influence the distances in the polyanionic network. However, there is no unambiguous answer to this question because the reduction of electron count is accompanied by a simultaneous change in the bonding polarity within the networks as well as a change in the unit cell volume (i.e. size of the network: larger for Mg compounds, smaller for Zn compounds). Comparing $AeZn_2X_2$ (X = Al, Ga) with the lowest bonding polarity and lowest volume change with the binary systems AeX_4 (X = Al, Ga) may reveal some information about how the reduction of the electron count from 14 to 12 affects the homonuclear X_a-X_a distances. The exchange of Al or Ga for Zn on the basal (X_b) position increases the Al_a-Al_a contacts by 0.02 Å (Ca) to 0.04 Å (Ba) and the Ga_a-Ga_a contacts by 0.02 Å (Ca) to 0.09 Å (Ba). For the pairs of Ca compounds $CaAl_4-CaZn_2Al_2$ and $CaGa_4-CaZn_2Ga_2$, where the X_a-X_a distances are least influenced by the Ae component, the reduction of electron count does not change the 2c2e bonding part in the network, but rather affects (weakens) multicenter bonding within the pyramids $X_a(X_b)_4$, which should reduce from 5c6e bonding to 5c5e bonding. However, it seems to be dangerous to associate bond orders/bond strengths with distances because of their flexibility in this particular case. The distances in the polyanionic network of most of the representatives with the $BaAl_4$ structure type are primarily determined by the size requirement of the Ae component.

General Stability Considerations. Following the ideas of Seo and Corbett[7] there are three factors governing the stability of s−p bonded compounds with the $BaAl_4$ structure: (1) the strength of the bonding in the polyanionic network (i.e. the covalent to polarized ionic interaction between X atoms); (2) the electrostatic interaction between Ae^{2+} and the polyanionic network $[X_4]^{2-}$; and (3) the size match between Ae and its encapsulating cage created by the polyanionic network. These factors are rather empirical (chemical) parameters and their quantification in terms of total energy contributions is, in general, not possible. Thus, the following discussion of structural stability of the $BaAl_4$-type compounds based on those parameters is comparative.

Table 3. SEN Values for Various $AeX1_2X2_2$ Systems Investigated

compds	SEN (AR)	SEN (Pauling)
$AeMg_{0.9}Al_{3.1}$	1.43	1.43
$AeMg_{1.7}Ga_{2.3}$	1.55	1.43
$AeMg_2Si_2$	1.45	1.50
$AeMg_2Ge_2$	1.60	1.50
$AeAl_2Zn_2$	1.60	1.55
$AeZn_{1.8}Ga_{2.2}$	1.76	1.60
$AeZn_2Si_2$	1.70	1.70
$AeZn_2Ge_2$	1.85	1.70

Network bonding: Clearly, the bonding strength in the networks is primarily determined by the electron count and the degree of bonding polarity. 14-Electron compounds possess an optimum electron count with all states filled up to the pseudogap. 12-Electron compounds appear electron deficient in this respect and thus network bonding is weaker. The change from homonuclear networks to heteronuclear ones is accompanied by the creation of polar (multicenter) bonding within pyramids $X_a(X_b)_4$. Usually polar bonds (between different partners) are stronger than homonuclear ones provided the bond order is not changed. With these considerations we may establish a sequence of relative network bond strengths: 12-electron ternary compounds < 14-electron binary compounds < 14-electron ternary compounds.

The nonexistence of the compounds $AeMg_2Al_2$ is surprising at first sight. Experimentally we found variable compositions for $SrMg_xAl_{4-x}$ and $BaMg_xAl_{4-x}$ with $x \leq$ ca. 0.9, i.e., compositions close to "$AeMgAl_3$." Compared to the corresponding Ga systems, where a much higher degree of Mg substitution is achieved (i.e. $AeMg_{1.7}Ga_{2.3}$), the DOS of $SrMg_2Ga_2$ and $BaMg_2Ga_2$ look very similar and no particular (inherent) reason (apart from the formation of competing, more favorable ternary compounds) for the instability of $SrMg_2Al_2$ or $BaMg_2Al_2$ is noticeable. However, a closer look at the DOS curves of the Ga systems reveal that the bands are more dispersed and also the Ga 4s bands are situated at a lower energy than the Al 3s bands in $AeMg_2Al_2$. This indicates that the interaction (bonding) between the network atoms is stronger in the Ga compounds and becomes too weak in the Al compounds. Empirically, we can express this fact by defining a minimum value for the (composition weighed) sum of the electronegativity, SEN, of the network atoms. For any composition $Ae(X1)_x(X2)_{4-x}$, SEN is calculated as

$$\mathrm{SEN} = [x(\mathrm{EN(X1)}) + (4 - x)(\mathrm{EN(X2)})]/4$$

and listed in Table 3. Large SEN values are associated with a high degree of covalency[44] and thus a high bonding strength in the polyanionic network. For $AeMg_xAl_{4-x}$ SEN takes the value 1.43 for the composition $x = 0.9$ (according to the Pauling and the Allred−Rochow EN scales, cf. Table 2). This value can be considered as a minimum value and is connected with the lowest bonding strength the polyanionic network can attain in a stable $BaAl_4$-type compound. For $AeMg_{1.7}Ga_{2.0.3}$ a SEN value of 1.43 (Pauling) or 1.54 (Allred-Rochow) is obtained, which suggests

(44) Allen, L. C.; Capitani, J. F.; Kolks, G. A.; Sproul, G. D. *J. Mol. Struct.* **1993**, *300*, 647.

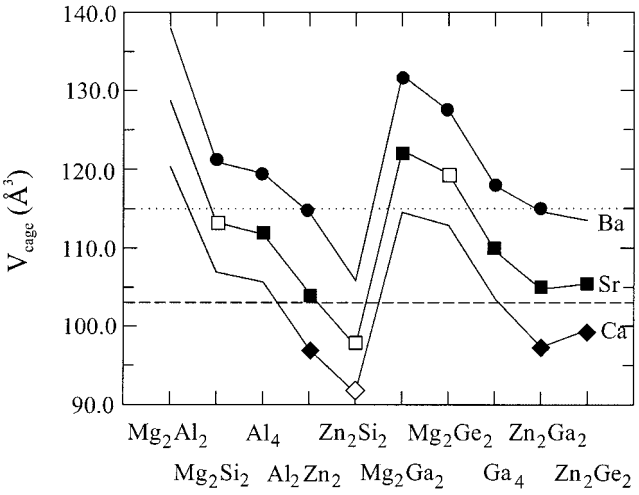

Figure 10. Compilation of the volumes of the Ae coordination Fedorov polyhedra (V_{cage}) in the investigated systems $Ae(X_b)_2(X_a)_2$ (calculated equilibrium structures). Solid symbols represent experimentally known compounds, open symbols indicate possibly existing compounds meeting the size match criterion for stable $BaAl_4$ compounds. The dotted line marks the lower size match boundary of Ba^{2+}, and the broken line marks the upper size match boundary of Ca^{2+}.

that they are at the borderline of minimum network bonding strength. We could corroborate this hypothesis by investigating the system $BaMg_xIn_{4-x}$. Indium has a comparable electronegativity to Al and we found the maximum content of Mg to be very close to that for the systems $SrMg_xAl_{4-x}$ and $BaMg_xAl_{4-x}$.[45]

Madelung interaction: The amount of stabilizing electrostatic interactions between Ae cations and the negative charge on the network sites is primarily determined by the network polarity and, to a minor extent, by the size of the network (i.e. the distances between cations and anions). Madelung energy calculations suggest that the amount of stabilizing electrostatic interactions increases with increasing charge separation on the network sites. Therefore, among the ternary 14- and 12-electron compounds, the electrostatic stabilization is larger than for the binary 14-electron compounds (especially for the Mg compounds with the highest network polarity). Consequently, 14-electron ternaries with an optimum electron count and the highest amount of Madelung interaction have the prerequisites for highest structural stability among the s−p bonded compounds with the $BaAl_4$ type.

Volume and size relations: The size match between electropositive Ae and the encapsulating cage formed by the network represents an important chemical parameter determining structural stability. We may simply define the volume of this cage as the volume of the Fedorov polyhedron[10] (Figure 1), which corresponds to half of the unit cell volume. The cage sizes as summarized in Figure 10 reveal an astonishing variability, which is basically due to the flexible 2c2e X_a-X_a contacts. For Ae = Ba the smallest cages occur in $BaAl_2Zn_2$ and $BaZn_2Ga_2$ (V = 115 Å^3), which probably represents the lower limit for matching the volume of Ba^{2+}. This is suggested by the nonlinear increase of the Zn_a-Zn_a distance in $AeAl_2Zn_2$ from Ae = Ca to Ba. Among the systems reported here, the largest cage volume for Ba^{2+} is obtained in $BaMg_2Ga_2$ (V = 132 Å^3). However, in $BaIn_4$[35] the cage size reaches 140 Å^3 and, thus, the size of Ba^{2+} matches a range of cage volumes from 115 Å^3 to at least 140 Å^3. For Ae = Ca, we propose that the cage size obtained in $CaAl_4$ and $CaGa_4$ (around 104 Å^3) is slightly above the upper limit and, thus, the tetragonal structure undergoes a monoclinic distortion. The stabilization gained by this distortion is very small. For $CaAl_4$ we obtained an energy difference of just 2 meV per formula unit between the tetragonal and monoclinic equilibrium structures, which is at the limit of accuracy of the applied theoretical method. For $CaGa_4$ this energy difference is 8 meV/formula unit. Importantly, the symmetry-lowering distortion leaves the equilibrium volume virtually unchanged because the network connectivity is not changed. For tetragonal $CaAl_4$ and $CaGa_4$ the network size is determined by the covalent, equilibrium bond lengths of the two different X_a-X_a and X_a-X_b contacts. As a consequence of the insufficient coordination (encapsulation) of Ca^{2+}, an electronic instability is introduced that drives a structural transition. Monoclinic $CaAl_4$ transforms to the tetragonal $BaAl_4$ type reversibly in a continuous way at 443 K, which was studied in detail by Miller et al.[13] For the (hypothetical) compounds "$CaMg_2Al_2$" and "$CaMg_2Ga_2$" with even larger unit cell volumes than $CaAl_4$ and $CaGa_4$, the cage sizes are too big for matching the volume of Ca^{2+}.

According to our results, Sr^{2+} matches a range of cage volumes from at least 103 Å^3 (in $SrZn_2Ge_2$) to at least 123 Å^3 ($SrMg_2Ga_2$). The upper limit for a Fedorov polyhedron based cage is exceeded in the newly discovered compound $SrIn_4$,[7] which adopts the monoclinic $EuIn_4$-type structure,[46] and Sr^{2+} is located in cages which are defined by five-membered rings rather than by six-membered ones as in the $BaAl_4$-type. Interestingly our recent experiments in the system $SrZn_xIn_{4-x}$ yielded the compound $SrIn_2Zn_2$ with the $BaAl_4$ structure.[45] The substitution of In by Zn leads to a considerable shrinkage of the unit cell, and enables Sr^{2+} again to match the size of the Fedorov polyhedron based cage, which has a volume of about 125 Å^3 in $SrIn_2Zn_2$. The system $SrZn_xIn_{4-x}$ further offers the possibility of determining the upper limit of the size match between Sr^{2+} volume of this kind of cage when the composition is more In rich. This is currently under investigation.

No representatives are yet reported for $AeZn_2Si_2$, which would generate the smallest unit cell volumes for these s−p $BaAl_4$-type systems. However, the cage size provided by $^3_\infty[Zn_2Si_2]^{2-}$ should be appropriate to match the volumes of Ca^{2+} and possibly also that of Sr^{2+}, so compounds $CaZn_2Si_2$ and $SrZn_2Si_2$ might actually exist, provided they are stable with respect to decomposition reactions in the ternary phase diagram. This holds also for compounds $SrMg_2Si_2$ and $SrMg_2Ge_2$. Compounds $BaZn_2Si_2$ and $BaZn_2Ge_2$, with too small cage sizes for Ba^{2+}, could probably be synthesized by high-pressure techniques; their DOS curves do not exhibit any electronic instability.

Site preference revised: In the ternary compounds the apical (X_a) network position is preferentially occupied by the element that forms the stronger homonuclear 2c2e contacts. The ability of an element to form strong 2c2e bonds scales with its electronegativity and, indeed, of the pair of network forming atoms, the more electronegative one occupies the five-coordinated X_a position. However, site preference as expressed by the coloring energy in Figure 2 is also influenced by the size of the Ae component. There is a linear decrease of the

(45) Häussermann, U., to be submitted for publication.

(46) Fornasini, M. L.; Cirafici, S. *Z. Kristallogr.* **1990**, *190*, 295−304.

coloring energy for most of the Mg-containing systems ($AeMg_2Si_2$, $AeMg_2Ge_2$, $AeMg_2Ga_2$, and $AeAl_2Zn_2$) with increasing size of Ae, while in others ($AeMg_2Al_2$, $AeZn_2Si_2$, $AeZn_2Ge_2$, and $AeZn_2Ga_2$) it is roughly independent of Ae. If the two networks $^3_\infty[X1_2X2_2]^{2-}$ and $^3_\infty[X2_2X1_2]^{2-}$ are either not influenced at all or both affected to the same degree by encapsulated Ae^{2+}, the coloring energy should not depend on the size of Ae. On the other hand, when the two networks are affected differently by Ae^{2+}, site preference becomes dependent on the size of Ae. Now, we can understand why site preference depends on Ae for most of the Mg systems, but does not for most of the Zn systems. In hypothetical $^3_\infty[X_2Mg_2]^{2-}$ networks with Mg on the apical position, the cage size for encapsulated Ae^{2+} is considerably larger compared to the more stable distributions $^3_\infty[Mg_2X_2]^{2-}$. This is because the X_a-X_a distance is quite long for $X_a = Mg$ (the X_a-X_b distances between multicenter bonded atoms are about the same in both networks). Thus, the size of Ae will not affect $^3_\infty[X_2Mg_2]^{2-}$ networks to the same extent as $^3_\infty[Mg_2X_2]^{2-}$ networks with smaller cages. On the other hand, cage sizes are not very different for $^3_\infty[Zn_2X_2]^{2-}$ and $^3_\infty[X_2Zn_2]^{2-}$ because the X_a-X_a distances are comparable for $X_a =$ Zn and p-element. Thus, the size of Ae affects both networks to about the same extent and the coloring energy is independent of Ae. This idea holds also for $AeMg_2Al_2$ and $AeAl_2Zn_2$, where the Zn compounds exhibit Ae-dependent site preference but the Mg compounds do not. The longest X_a-X_a contacts occur for Al whereas Zn expresses rather short X_a-X_a bonds. Therefore, the $^3_\infty[Al_2Zn_2]^{2-}$ network provides a smaller cage than the $^3_\infty[Zn_2Al_2]^{2-}$ network, and is more affected by the size of the encapsulated Ae^{2+}. On the other hand, cage sizes for $AeMg_2Al_2$ are about the same for both distributions and the coloring energy is not very dependent on the Ae component.

A final important question concerning site preference is at which coloring energy will mixed occupancy on the network sites take place. The $AeAl_2Zn_2$ system provides insight into this question: the onset of mixed occupancy occurs for a coloring energy around 0.38 eV/formula unit as in $CaAl_2Zn_2$ (10% mixed occupancy) and increases to at least 25% for a coloring energy of 0.17 eV/formula unit as in $BaAl_2Zn_2$. This suggests that $CaZn_2Ge_2$ and $SrZn_2Ge_2$, which were reported as completely ordered, actually may have a considerable degree of mixed occupancy because the (Ae independent) coloring energy is just around 0.23 eV/formula unit.

Conclusions

The large family of polar intermetallic compounds is distinguished by an exceptionally rich variety of different structures, which accompanies the transition from the nonmetallic to the metallic state. Structural stability of polar intermetallics involves a complicated interplay among different factors. We have analyzed in detail variations of the electronic and atomic structures in the s−p bonded, $BaAl_4$-type polar intermetallics, $AeX(III)_4$, $AeX(II)_2X(IV)_2$, and $AeX(II)_2X(III)_2$ (Ae = Ca, Sr, Ba; X(III) = Al, Ga, In; X(II) = Mg, Zn; X(III) = Si, Ge). Their structure is composed of an Ae^{2+} cation that is encapsulated by a polyanionic $^3_\infty[X_4]^{2-}$ network featuring localized 2c2e as well as delocalized multicenter bonding. Compared to Zintl phases, which can be described by localized bonding within the polyanionic framework, there are two main differences concerning the factors governing the formation of these polar intermetallic $BaAl_4$-type structures:[47] (i) there is a considerable weakening of the status of valence electron count as the predominant structure determining parameter and (ii) the polyanionic network can readily adapt to differently sized cations without structural change. Although the optimum electron count of s−p bonded $BaAl_4$-type systems is 14 electrons per formula unit, which separates network bonding states from antibonding states by a pseudo-gap in the DOS, there do exist an extensive number of 12-electron examples with electron-deficient network bonding. As valence electron count changes in Zintl phases (by chemical substitution), the connectivity within the polyanionic network changes. Furthermore, the flexibility of the polyanionic framework in these $BaAl_4$-type examples is evident by the nearly 15% increase in volume for $AeAl_2Zn_2$ and $AeZn_2Ga_2$ between Ae = Ca and Ba. This flexibility also is in contrast to Zintl phase networks in which the size of the cages provided for the cations is rather rigid and typically a particular polyanionic network cannot match an extended series of differently sized cations.

Acknowledgment. This work was supported by the Swedish National Science Research Council (NFR), the Göran Gustafsson Foundation, and the National Science Foundation through NSF DMR 99-81766. We would like to thank J. Garcia (Stockholm University) for valuable assistance with the electron microscopes.

Supporting Information Available: Data collection and refinement parameters, atomic coordinates, interatomic distances, and structural parameters and binding energies obtained for the computationally obtained, equilibrium structures (PDF). This material is available free of charge via the Internet at http://pubs.acs.org.

JA012392V

(47) Kauzlarich, S. M., Ed. *Chemistry, Structure and Bonding of Zintl Phases and Ions*; VCH: New York, 1996.